## ABSTRACT

*Positron emission tomography (PET) is a sensitive technique for functional and molecular imaging. In Japan, the incidence of cognitive disorders is increasing at an accelerated pace, partly due to the increasing size of the elderly population. Basic and clinical studies on dementia have become very important. In vivo detection of amyloid beta (Aβ) deposits could be useful for early diagnosis of Alzheimer's disease (AD). "Aβ imaging" by PET has been recognized as one of the most important methods for the early diagnosis of AD. Clinical PET studies have been conducted using several probes, such as [$^{18}$F]FDDNP, [$^{11}$C]SB-13 and [$^{11}$C]Pittsburgh compound-B ([$^{11}$C]PIB). [$^{11}$C]PIB is the most commonly used probe.*

*In this chapter, a novel imaging probe, 2-[2-(2-dimethylaminothiazol-5-yl)-ethenyl]-6- [2-(fluoro)ethoxy] benzoxazole ([$^{11}$C]BF-227), is reported. To the authors' knowledge, [$^{11}$C]BF-227 is the first Aβ imaging probe to be used in Japan. The purpose of this chapter is to examine methods for quantitative analysis of Aβ deposition in the human brain using PET and [$^{11}$C]BF-227. Six AD patients and six healthy control subjects were used in the present study. Dynamic PET images were obtained over 60 min. Blood samples were obtained from the radial arteries.*

*The results were analyzed using Logan graphical analysis and full kinetic analysis. A significantly higher distribution volume ratio (DVR) value was observed in AD patients in cortical regions, e.g., the cingulate, frontal, temporal, parietal and occipital regions, than in control subjects. Satisfactory correlation of these values to the semiquantitative standardized uptake values (SUV) was obtained.*

*These findings suggest that [$^{11}$C]BF-227 is a promising PET probe for clinical evaluation of early Aβ deposition in AD patients.*

## INTRODUCTION

### Positron Emission Tomography

Positron emission tomography (PET) is a technique used for functional and molecular imaging based on nuclear medicine technology. Nuclear medicine techniques date back to the early 20th century. Nuclear medicine was originally developed as a "tracer technique" by the Nobel laureate, Dr. George de Hevesy. In our study, the term "tracer" means an extremely small amount of radioisotope that is administered to the subject to permit imaging certain biological phenomena in the living body. A tracer is sometimes also called a "probe". Probes detect the presence of a certain biological substances in small amounts (often at the "nano-" to "pico-" molar scale) (Tashiro, 2010). The tracer technique was later established as a nuclear medicine technique in the late 20th century, mainly due to advancements in radiolabeling techniques and signal detection devices such as PET.

Using PET, a wide range of biological information can be obtained from the living human brain, such as the cerebral metabolic rate of glucose (CMRglc), regional cerebral blood flow (rCBF) and pharmacokinetic information regarding receptor-transmitter interactions such as those in the dopaminergic and histaminergic neuronal systems (Yanai & Tashiro, 2007; Tashiro, 2010). CMRglc is often measured using a radioactive analogue of glucose, [$^{18}$F]fluorodeoxyglucose ([$^{18}$F]FDG). In brain regions that have increased glucose consumption, an increased demand for glucose and oxygen causes dilation of cerebral capillaries, which can be measured as an increase in the regional cerebral blood flow (rCBF)(Tashiro, 2008). The rCBF is measured using radiolabeled water ([$^{15}$O]$H_2O$), though other radiation-free

techniques, such as functional magnetic resonance imaging (fMRI) and near-infrared light spectroscopy (NIRS), are also available. Currently, PET is useful for visualization and quantification of various molecular phenomena, such as neurotransmission, DNA synthesis, and production of physiological and pathological proteins, in living organisms. To our knowledge, PET is one of the most sensitive imaging techniques. (Figure 1)

In Japan, the incidence of cognitive disorders is increasing at an accelerated pace, partly due to the increasing size of the elderly population. Basic and clinical studies on dementia have become increasingly important. In functional neuroimaging of early Alzheimer's disease (AD), it is commonly known that a decrease in the $CMR_{glc}$ often starts in the posterior cingulate gyrus and propagates to the temporo-parietal and other regions, as visualized by [$^{18}$F]FDG PET (Minoshima, 1994; Furukawa, 2009; Ishii, 2009). In this stage of dementia, many nerve cells are damaged and the density of healthy neurons is reduced in the gray matter, resulting in low [$^{18}$F]FDG uptake. However, the regional metabolic reduction is not easily detected and is widespread during early disease stages, e.g., mild cognitive impairment (MCI)(Furukawa, 2009; Ishii, 2009). Neuronal damage is associated with high deposition of amyloid β (Aβ) protein in the brain, and massive neuronal loss is often preceded by high Aβ deposition. An early diagnosis of mild AD can be established if a tracer that specifically binds to Aβ proteins is used.

## Amyloid β Imaging with PET

"Aβ imaging" using PET and an Aβ-specific probe has been recognized as one of the most important methods for the diagnosis of early AD. This is, in part, due to the excellent sensitivity of the PET

*Figure 1. Information available from the human brain. Information regarding glucose and oxygen metabolism obtained using [$^{18}$F]FDG PET and [$^{15}$O]$O_2$ PET. Currently, regional cerebral blood flow is measured using various methods, such as [$^{15}$O]$H_2O$ PET, functional MRI (fMRI) and near infrared light spectroscopy (NIRS). Interaction of neurotransmitters and receptors is measured using PET and various radiotracers labeled with $^{18}$F and $^{11}$C nuclides.*

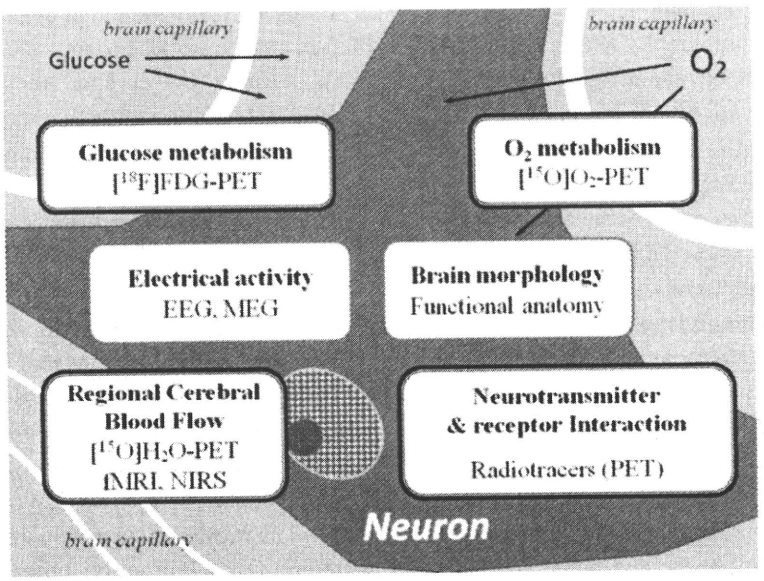

technique (Nordberg, 2004). It is important that Aβ deposition detection occur as soon as possible to allow initiation of medication before the symptoms of dementia worsen. It is believed that deposition and aggregation of Aβ begins before patients manifest clinical symptoms. Numerous candidate compounds have been tested for Aβ imaging, and several compounds were selected for clinical studies (Furumoto, 2007). Clinical PET studies have been conducted using several probes, such as [$^{18}$F]FDDNP (Shoghi-Jadid, 2002), [$^{11}$C]SB-13 (Verhoeff, 2004), and [$^{11}$C]Pittsburgh compound-B ([$^{11}$C]PIB)(Klunk, 2004), in addition to others (Figure 2). Among these compounds, [$^{11}$C]PIB is the most commonly used (Klunk, 2004; Mintun, 2005; Price, 2005). Many studies have clearly demonstrated that [$^{11}$C]PIB binds to Aβ fibrils, enabling noninvasive assessment of Aβ deposition in the brain of AD patients (Klunk, 2004).

Considering the importance of Aβ imaging, our group developed a novel PET tracer, 2-(2-[2-demethylaminothiazol-5-yl] ethenyl)-6-(2-[Fluoro]ethoxy)benzoxazole (BF-227), which is the first compound used for human studies in Japan (Kudo, 2007). Our clinical study demonstrated that this compound is able to detect Aβ deposition primarily in the posterior association area of AD patients. Accumulation in the frontal area is not prominent (Kudo, 2007). Interestingly, in contrast to [$^{11}$C]PIB, [$^{11}$C]BF-227 preferentially detects senile plaques containing dense amyloid fibrils. This provides unique and specific information regarding Aβ pathology in AD patients (Kudo, 2007). In addition, we compared the ability of [$^{11}$C]BF-227 PET, structural MRI, and FDG PET to diagnose and track the severity of AD. [$^{11}$C]BF-227 PET was more sensitive than MRI in the diagnosis of AD and the detection of converters from MCI to AD (Waragai, 2009). These studies indicate that [$^{11}$C]BF-227 PET is a useful method for the early diagnosis of AD and prediction of converters from MCI to AD (Furukawa, 2009; Waragai, 2009).

Though these PET studies succeeded in establishing [$^{11}$C]BF-227 as a useful tracer, they used standardized uptake values (SUV) as a tool for clinical evaluation. This is a semi-quantitative measure that corrects for the injected dose and body size of the subject. Precise quantitative examination may provide a better rationale for the use of this method as a clinical tool, similar to studies of [$^{11}$C]PIB (Mintun, 2005; Price, 2005). However, we have not conducted the precise examination of [$^{11}$C]BF-227 pharmacokinetics in the human brain using data from arterial samples. In this paper,

*Figure 2. Chemical structures of amyloid imaging agents, FDDNP, SB-13, PIB, and BF-227*

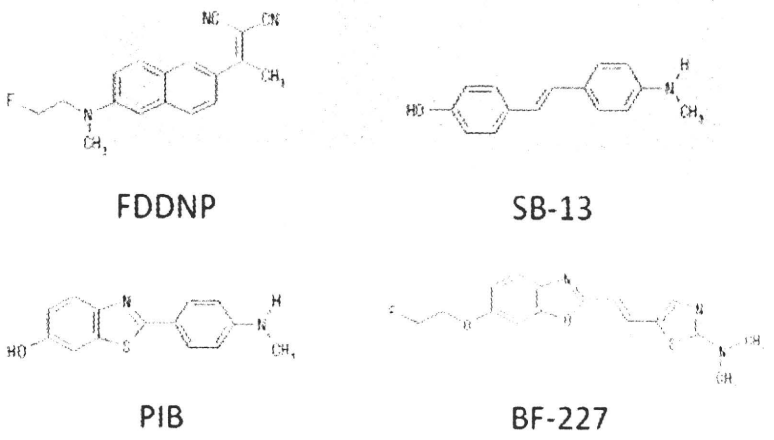

quantification methods for Aβ imaging with PET are briefly overviewed and the preliminary results of the [$^{11}$C]BF-227 PET study are discussed.

## MATERIALS AND METHODS

### Subjects

In the present study, 6 AD patients (mean age: 73 years) and 6 healthy volunteers (mean age: 61 years) were recruited. PET scans were initiated simultaneously with [$^{11}$C]BF-227 injection and data from 23 time frames (30 sec×5, 60 sec×5, 150 sec×5, 300 sec×8) were obtained. Serial arterial blood sampling was also performed (10 sec×12, 20 sec×3, 60 sec×2, 150 sec×2, 300 sec×2, 600 sec×4). The metabolite fraction in the blood was also examined at 5, 15, 30 and 60 min post-injection, and the fraction data were used for correction of input functions. PET data were co-registered to the individual MRI T1 images to define regions of interest (ROIs) in the cortex and subcortical deep nuclei (Figure 3a,b).

This study was approved by the ethics committee of Tohoku University Graduate School of Medicine, and informed consent was obtained from each subject.

### Method

The distribution volume (DV) and binding potential (BP) values of [$^{11}$C]BF-227 were estimated using a full kinetic compartmental model based on the 1-tisssue (1TM) and 2-tissue models (2TM) (Figure 3d). Graphical analysis methods were also applied using 2 types of Logan graphical analysis; one used the time-activity curve (TAC) of arterial plasma data as an input function for analysis (LGA)(Logan, 1990) and the other used

*Figure 3. Regions of interest (ROIs) defined in the cerebral cortex and subcortical deep nuclei of a healthy volunteer subject taken by MRI (a) and the co-registered PET (b). The results of linearization using Logan graphical analysis (c) and time activity curves in plasma and brain tissue for compartmental model analysis (d) are demonstrated.*

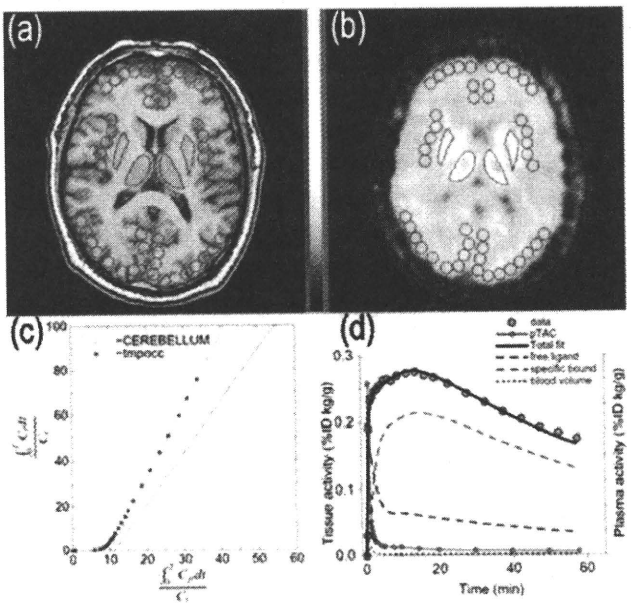

the TAC of reference brain tissue (cerebellum) (LGAR) (Logan, 1996) (Figure 3c). PMOD software (version 3.0; PMOD Technologies, Zurich, Switzerland) was used for calculation. The results of the compartmental model analysis and graphical analysis were compared to the SUV and the SUV ratios of the cerebellar SUV (cerebellar SUVR). Correlations derived from these different methods were examined.

## RESULTS

The plasma TAC was not different between AD patients and control subjects. However, a difference was observed in the tissue TAC between AD patients and control subjects. [$^{11}$C]BF-227 accumulation was significantly higher in the cerebral cortex than in the cerebellum of AD patients, whereas there was no difference in control subjects (Figure 4).

Our analysis determined that the 2TM described the pharmacokinetics of [$^{11}$C]BF-227 better than 1TM (Figure 5). The DV and BP values of [$^{11}$C]BF-227 were significantly higher in AD patients than in control subjects, and the most prominent difference was observed in the temporo-occipital and lateral temporal regions. The DV values from the 2TM and LGA ($r^2$ >0.95 in all regions) methods were similar. In addition, the results of LGA and LGAR were also similar, and the LGA values were similar to the SUV and cerebellar SUVR ($r^2$ >0.94 in all regions).

## DISCUSSION

Currently, Aβ imaging using PET has been recognized as one of the most effective methods for diagnosing early AD and for predicting potential converters from MCI to AD (Nordberg, 2004; Klunk, 2006). Several promising probes, such as [$^{18}$F]FDDNP (Shoghi-Jadid, 2002), [$^{11}$C]SB-13

*Figure 4. Time activity curves (TAC) of the cerebral cortex and cerebellum of healthy controls (Control) and Alzheimer's disease patients (AD patient). Open circles indicate TAC in the cerebellum and closed squares indicate TAC in the cerebral cortical tissues, e.g., the temporo-occipital cortex (temp-occ) and lateral temporal cortex (ltm). [$^{11}$C]BF-227 accumulation was significantly higher in the cerebral cortex than in the cerebellum of AD patients, whereas there was no difference in control subjects.*

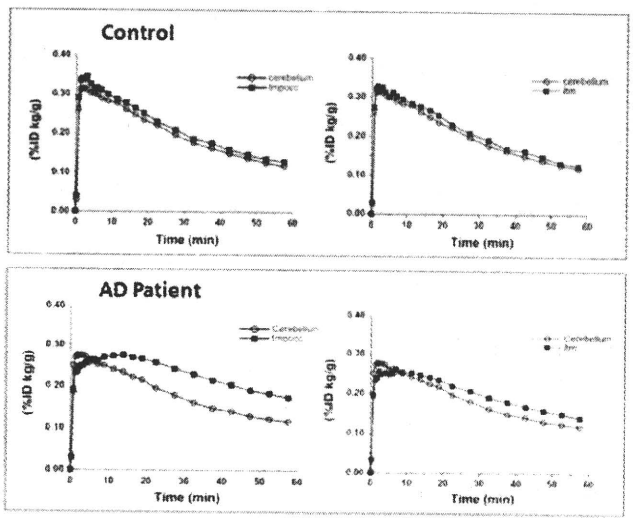

*Figure 5. Analysis of the time-activity curve in the temporoparietal cortex of an Alzheimer's disease patient based on the 1-tissue (LEFT) and 2-tissue compartmental models (RIGHT). The 2-tissue model gave more accurate results.*

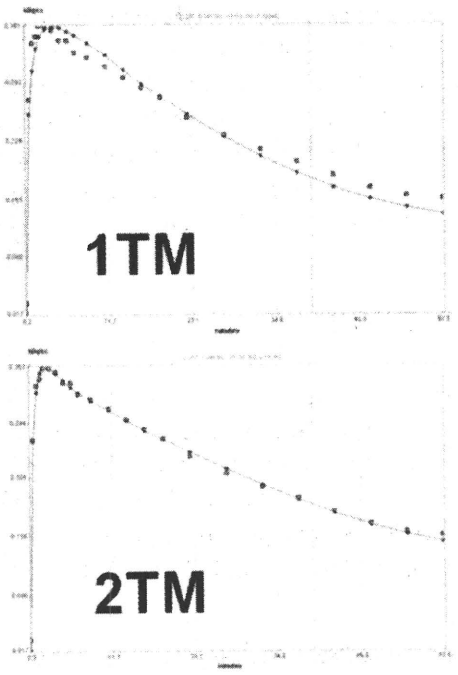


(Verhoeff, 2004) and [$^{11}$C]PIB (Klunk, 2004), have been tested in clinical studies, and [$^{11}$C]PIB is regarded as the most successful Aβ imaging probe. Though an initial study was performed without arterial blood sampling and mainly used SUV for clinical evaluation (Klunk, 2004), the results of a quantitative study were reported in detail (Price, 2005).

Initial studies using [$^{11}$C]BF-227 have been conducted in a similar manner. Kudo and colleagues reported that this compound was able to detect Aβ deposition primarily in the posterior association area of AD patients, suggesting that [$^{11}$C] BF-227 may be able to preferentially detect senile plaques containing dense amyloid fibrils. This is in contrast to [$^{11}$C]PIB, which provides unique and specific information regarding Aβ pathology in AD patients (Kudo, 2007). In addition, we performed a comparative study between [$^{11}$C]BF-227 PET and structural MRI for the diagnosis and tracking of AD pathology. The results demonstrated that PET with [$^{11}$C]BF-227 was more sensitive than MRI for detection of voxel-based morphometry (VBM) (Waragai, 2009). Another study demonstrated that [$^{11}$C]BF-227 was more sensitive than FDG PET for diagnosis of AD and detection of converters from MCI to AD (Furukawa, 2009). Thus, these studies suggest that Aβ PET imaging is more sensitive than detection of hippocampal atrophy and reduced metabolism of glucose.

The pharmacokinetics of [$^{11}$C]PIB have been thoroughly examined using various quantification methods, such as full kinetic analysis and graphical analysis (Mintun, 2005; Price, 2005). In full kinetic analysis, the commonly used compartmental models are the 3-compartment model (2-tissue compartmental model: 2TM), in which one blood compartment and 2 tissue compartments with specific and non-specific binding are assumed (Figure 6), and the 2-compartmental model (1-tissue compartmental model: 1TM), in which one tissue compartment represents both specific and non-specific binding (Mintun, 2005; Price, 2005). When the tracer rapidly penetrates the blood-brain barrier (BBB) in the tissue compartment, the 1-tissue compartmental model is more appropriate for describing its kinetics. In the analysis of [$^{11}$C]PIB, 2TM is more appropriate for describing the kinetics of tracer binding to Aβ in the human brain (Mintun, 2005; Price, 2005). Price and colleagues reported that Logan graphical analysis (LGA) was more useful and robust than 2TM analysis. However, in the cerebellum, in which the reference regions are assumed to be free of mature Aβ plaques, 2TM analysis was more appropriate (Price, 2005). Though many [$^{11}$C]PIB studies employ DVR values for clinical evaluation, the use of BP was also proposed in the paper by Mintun and colleagues (Mintun, 2005).

Similar to [$^{11}$C]BF-227, compartmental analysis indicated that 2TM analysis was a better

*Figure 6. Basic compartmental models describing the distribution and binding of radiotracers: 2-tissue model (TOP) and 1-tissue model (BOTTOM). Abbreviations: $C_p$, plasma concentration; $C_{f+ns}$, concentration of free and nonspecifically bound tracers in the brain tissue; $C_b$, concentration of specifically bound tracers in the brain tissue.*

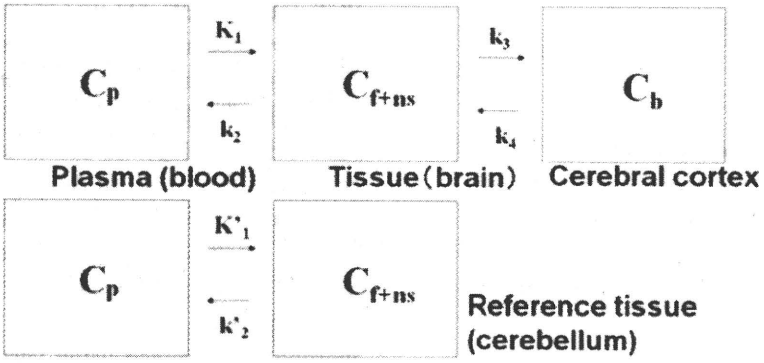


fit than 1TM when analyzing data from [$^{11}$C]PIB (Price, 2005). Linearization by the LGA method was also successful when analyzing the [$^{11}$C]PIB data. A significant correlation between the DV values calculated by 2TM and LGA analysis (and LGAR, as well) suggests that Logan methods are fully applicable to the quantification of [$^{11}$C]BF-227. A significant correlation of the results of Logan methods to the SUV (and SUVR) suggests that clinical evaluation of Aβ deposition using [$^{11}$C]BF-227 PET is possible using LGA (and LGAR), SUV, and SUVR. These results reconfirm the reliability of the results from our recent studies (Kudo, 2007; Furukawa, 2009; Waragai, 2009).

In summary, we demonstrated that [$^{11}$C]BF-227 is a promising tracer for Aβ imaging, diagnosing AD patients and detecting potential converters from MCI to AD. In addition to the study on AD diagnosis, recent clinical applications of [$^{11}$C] BF-227 PET have successful. For instance, PET imaging was used to visualize pathological prion proteins in prion diseases (Okamura, 2009) and to image α-synuclein deposition in multiple system atrophy (Kikuchi, 2010).

Future studies should be performed to obtain more accurate data. However, correction for the partial volume effect should be considered. This partial volume correction (PVC) is important because of local atrophy in AD patients and the relatively high accumulation of [$^{11}$C]BF-227 in the white matter, as observed using [$^{11}$C]PIB PET (Meltzer, 1999; Price, 2005). A practical correction method has been proposed for the analysis of [$^{11}$C] PIB data, and it was demonstrated that the difference of the results with and without PVC correction was negligible in [$^{11}$C]PIB PET (Meltzer, 1999; Price, 2005). In future studies, development of a simplified protocol will be important. Omission of serial blood sampling is practical and would be helpful for clinical use. In a [$^{11}$C]PIB PET study, Lopresti and colleagues demonstrated that the TAC taken from the ROIs of bilateral carotid arteries defined in MRI co-registered PET images could be successfully used as an input function to obtain reliable results with acceptable errors (Lopresti, 2005).

## ACKNOWLEDGMENT

This study was partly supported by grant-in-aids from the Ministry of Health, Welfare and Labor for Amyloid imaging and a grant for education and research for molecular imaging (JST). The

authors thank to all the staff of the Cyclotron and Radioisotope Center, Tohoku University for the operation of the cyclotron and administering of patient care.

## REFERENCES

Furukawa, K., Okamura, N., Tashiro, M., Waragai, M., Furumoto, S., & Iwata, R. (2009). Amyloid PET in mild cognitive impairment and Alzheimer's disease with BF-227: Comparison to FDG-PET. *Journal of Neurology, 257*, 721–727. doi:10.1007/s00415-009-5396-8

Furumoto, S., Okamura, N., Iwata, R., Yanai, K., Arai, H., & Kudo, Y. (2007). Recent advances in the development of amyloid imaging agents. *Current Topics in Medicinal Chemistry, 7*, 1773–1789. doi:10.2174/156802607782507402

Ishii, H., Ishikawa, H., Meguro, K., Tashiro, M., & Yamaguchi, S. (2009). Decreased cortical glucose metabolism in converters from CDR 0.5 to Alzheimer's disease in a community: The Osaki-Tajiri Project. *International Psychogeriatrics, 21*, 148–156. doi:10.1017/S1041610208008132

Kikuchi, A., Takeda, A., Okamura, N., Tashiro, M., Hasegawa, T., & Furumoto, S. (2010). In vivo visualization of α-synuclein deposition by carbon-11-labeled 2-(2-[2-dimethylaminothiazol-5-yl]ethenyl)-6-(2-[fluoro]ethoxy)benzoxazole positron emission tomography in multiple system atrophy. *Brain, 133*, 1772–1778. doi:10.1093/brain/awq091

Klunk, W. E., Engler, H., Nordberg, A., Wang, Y., Blomqvist, G., & Holt, D. P. (2004). Imaging brain amyloid in Alzheimer's disease with Pittsburgh Compound-B. *Annals of Neurology, 55*, 306–319. doi:10.1002/ana.20009

Klunk, W. E., Mathis, C. A., Price, J. C., Lopresti, B. J., & DeKosky, S. T. (2006). Two-year follow-up of amyloid deposition in patients with Alzheimer's disease. *Brain, 129*, 2805–2807. doi:10.1093/brain/awl281

Kudo, Y., Okamura, N., Furumoto, S., Tashiro, M., Furukawa, K., & Maruyama, M. (2007). 2-(2-[2-Dimethylaminothiazol-5-yl]ethenyl)-6-(2-[fluoro]ethoxy)benzoxazole: A novel PET agent for in vivo detection of dense amyloid plaques in Alzheimer's disease patients. *Journal of Nuclear Medicine, 48*, 553–561. doi:10.2967/jnumed.106.037556

Logan, J., Fowler, J. S., Volkow, N. D., Wang, G. J., Ding, Y. S., & Alexoff, D. L. (1996). Distribution volume ratios without blood sampling from graphical analysis of PET data. *Journal of Cerebral Blood Flow and Metabolism, 16*, 834–840. doi:10.1097/00004647-199609000-00008

Logan, J., Fowler, J. S., Volkow, N. D., Wolf, A. P., Dewey, S. L., & Schlyer, D. J. (1990). Graphical analysis of reversible radioligand binding from time-activity measurements applied to [N-11C-methyl]-(-)-cocaine PET studies in human subjects. *Journal of Cerebral Blood Flow and Metabolism, 10*, 740–747.

Lopresti, B. J., Klunk, W. E., Mathis, C. A., Hoge, J. A., Ziolko, S. K., & Lu, X. (2005). Simplified quantification of Pittsburgh Compound B amyloid imaging PET studies: A comparative analysis. *Journal of Nuclear Medicine, 46*, 1959–1972.

Meltzer, C. C., Kinahan, P. E., Greer, P. J., Nichols, T. E., Comtat, C., & Cantwell, M. N. (1999). Comparative evaluation of MR-based partial-volume correction schemes for PET. *Journal of Nuclear Medicine, 40*, 2053–2065.

Minoshima, S., Foster, N. L., & Kuhl, D. E. (1994). Posterior cingulate cortex in Alzheimer's disease. *Lancet, 344*, 895. doi:10.1016/S0140-6736(94)92871-1

Mintun, M. A. (2005). Utilizing advanced imaging and surrogate markers across the spectrum of Alzheimer's disease. *CNS Spectrums, 10*, 13–16.

Nordberg, A. (2004). PET imaging of amyloid in Alzheimer's disease. *The Lancet Neurology, 3*, 519–527. doi:10.1016/S1474-4422(04)00853-1

Okamura, N., Shiga, Y., Furumoto, S., Tashiro, M., Tsuboi, Y., & Furukawa, K. (2009). In vivo detection of prion amyloid plaques using [(11) C]BF-227 PET. *European Journal of Nuclear Medicine and Molecular Imaging, 37*, 934–941. doi:10.1007/s00259-009-1314-7

Price, J. C., Klunk, W. E., Lopresti, B. J., Lu, X., Hoge, J. A., & Ziolko, S. K. (2005). Kinetic modeling of amyloid binding in humans using PET imaging and Pittsburgh Compound-B. *Journal of Cerebral Blood Flow and Metabolism, 25*, 1528–1547. doi:10.1038/sj.jcbfm.9600146

Shoghi-Jadid, K., Small, G. W., Agdeppa, E. D., Kepe, V., Ercoli, L. M., & Siddarth, P. (2002). Localization of neurofibrillary tangles and beta-amyloid plaques in the brains of living patients with Alzheimer disease. *The American Journal of Geriatric Psychiatry, 10*, 24–35.

Tashiro, M., Itoh, M., Fujimoto, T., Masud, M. M., Watanuki, S., & Yanai, K. (2008). Application of positron emission tomography to neuroimaging in sports sciences. *Methods (San Diego, Calif.), 45*, 300–306. doi:10.1016/j.ymeth.2008.05.001

Tashiro, M., Miyake, M., Masud, M. M., Ogura, M., Watanuki, S., & Yanai, K. (2010). Nano-bio-imaging with radiopharmaceuticals and its application to health sciences. *Annals of nanoBME, 3*, 73-87.

Verhoeff, N. P., Wilson, A. A., Takeshita, S., Trop, L., Hussey, D., & Singh, K. (2004). In-vivo imaging of Alzheimer disease beta-amyloid with [11C] SB-13 PET. *The American Journal of Geriatric Psychiatry, 12*, 584–595.

Waragai, M., Okamura, N., Furukawa, K., Tashiro, M., Furumoto, S., & Funaki, Y. (2009). Comparison study of amyloid PET and voxel-based morphometry analysis in mild cognitive impairment and Alzheimer's disease. *Journal of the Neurological Sciences, 285*, 100–108. doi:10.1016/j.jns.2009.06.005

Yanai, K., & Tashiro, M. (2007). The physiological and pathophysiological roles of neuronal histamine: An insight from human positron emission tomography studies. *Pharmacology & Therapeutics, 113*, 1–15. doi:10.1016/j.pharmthera.2006.06.008

## KEY TERMS AND DEFINITIONS

**[$^{11}$C]BF-227:** The first radiolabeled compound used for PET Aβ imaging in Japan.

**[$^{11}$C]Pittsburgh Compound-B ([$^{11}$C]PIB):** The most common radiolabeled compound used for PET imaging of Amyloid β.

**Amyloid β Imaging (Aβ Imaging):** A method for the early diagnosis of mild AD using a probe that specifically binds to Aβ proteins in vivo.

**Full Kinetic Analysis:** A type of mathematical technique used to estimate pharmacokinetic properties of radiolabeled tracers in biological organisms. This is an accurate method; however, the analytic procedure is sometimes complex and time-consuming. This is partly because this method uses non-linear analysis based on the minimum square method. Therefore, an appropriate compartmental model should be selected in advance.

**Logan Graphical Analysis:** A type of mathematical technique used to estimate pharmacokinetic properties of radiolabeled tracers in biological organisms. This method is convenient because a proper compartmental model is not required. Results are plotted as the distribution volume value.

**Neuroimaging:** Use of various techniques to either directly or indirectly image the structure

and function/pharmacology of the brain. It is a relatively new discipline within the medicine and neuroscience/psychology communities.

**Neuroscience:** The scientific study of the nervous system.

**Positron Emission Tomography (PET):** A functional and molecular neuroimaging technique based on nuclear medicine technology that measures various types of biological information, such as regional cerebral metabolic rate for glucose, cerebral blood flow and pharmacology.

# Early Detection and Rehabilitation Technologies for Dementia:

## Neuroscience and Biomedical Applications

Jinglong Wu
*Okayama University, Japan*

Medical Information Science
REFERENCE

| | |
|---|---|
| Senior Editorial Director: | Kristin Klinger |
| Director of Book Publications: | Julia Mosemann |
| Editorial Director: | Lindsay Johnston |
| Acquisitions Editor: | Erika Carter |
| Development Editor: | Myla Harty |
| Production Coordinator: | Jamie Snavely |
| Typesetters: | Mike Brehm, Jennifer Romanchak and Deanna Jo Zombro |
| Cover Design: | Nick Newcomer |

Published in the United States of America by
Medical Information Science Reference (an imprint of IGI Global)
701 E. Chocolate Avenue
Hershey PA 17033
Tel: 717-533-8845
Fax: 717-533-8661
E-mail: cust@igi-global.com
Web site: http://www.igi-global.com/reference



Library of Congress Cataloging-in-Publication Data

Early detection and rehabilitation technologies for dementia: neuroscience and biomedical applications / Jinglong Wu, editor.
p. ; cm.
Includes bibliographical references and index.
Summary: "This book provides a comprehensive collection for experts in the Neuroscience and Biomedical technology fields, outlining various concepts from cognitive neuroscience and dementia to neural technology and rehabilitation"--Provided by publisher.
ISBN 978-1-60960-559-9 (hardcover) -- ISBN 978-1-60960-560-5 (ebook) 1. Dementia--Diagnosis. 2. Neurologic examination. I. Wu, Jinglong, 1958-
[DNLM: 1. Dementia. 2. Brain--physiopathology. 3. Diagnostic Techniques, Neurological. 4. Early Diagnosis. WM 220]
RC521.E27 2011
616.8'3--dc22
2010054442

British Cataloguing in Publication Data
A Cataloguing in Publication record for this book is available from the British Library.

# Chapter 28
# Noninvasive Detection of Misfolded Proteins in the Brain Using [$^{11}$C]BF-227 PET

**Nobuyuki Okamura**
*Department of Pharmacology, Tohoku University, Japan*

**Hiroyuki Arai**
*Institute of Development, Aging and Cancer, Tohoku University, Japan*

**Shozo Furumoto**
*Department of Pharmacology & Cyclotron and Radioisotope Center, Tohoku University, Japan*

**Yukitsuka Kudo**
*Innovation of New Biomedical Engineering Center, Tohoku University, Japan*

**Manabu Tashiro**
*Cyclotron and Radioisotope Center, Tohoku University, Japan*

**Kazuhiko Yanai**
*Department of Pharmacology, Tohoku University, Japan*

**Katsutoshi Furukawa**
*Institute of Development, Aging and Cancer, Tohoku University, Japan*

## ABSTRACT

*Alzheimer's disease (AD) and many other neurodegenerative disorders belong to the family of protein misfolding diseases. These diseases are characterized by the deposition of insoluble protein aggregates containing an enriched β-sheet structure. To evaluate PET amyloid-imaging tracer [$^{11}$C]BF-227 as an agent for in vivo detection of various kinds of misfolded protein, a [$^{11}$C]BF-227 PET study was performed in patients with various protein misfolding diseases, including AD, frontotemporal dementia (FTD), dementia with Lewy bodies (DLB), sporadic Creutzfeldt-Jakob disease (sCJD) and Gerstmann-Sträussler-Scheinker disease (GSS). BF-227 binds to β-amyloid fibrils with high affinity. Most of the AD patients showed prominent retention of [$^{11}$C]BF-227 in the neocortex. In addition, neocortical retention of BF-227 was observed in the subjects with mild cognitive impairment who converted to AD during*

DOI: 10.4018/978-1-60960-559-9.ch028

*follow-up. DLB patients had elevated [$^{11}$C]BF-227 uptake in the neocortex. However, FTD and sCJD patients showed no cortical retention of [$^{11}$C]BF-227. Patients with multiple system atrophy had elevated BF-227 binding in the putamen. Finally, GSS patients had elevated BF-227 uptake in the cerebellum and other brain regions. This chapter confirms that BF-227 can selectively bind to α-synuclein and prion protein deposits using postmortem brain samples. Based on these findings, [$^{11}$C]BF-227 is not necessarily specific for β-amyloid in AD patients. However, this tracer could be used to detect various types of protein aggregates in the brain.*

## INTRODUCTION

Alzheimer's disease (AD) is the most common cause of dementia in the elderly. AD currently affects 4 million people in the United States and 15 million people globally. This disease begins insidiously with mild memory problems and progresses to the development of functional impairment in multiple cognitive domains within a few years. It is important to develop diagnostic methods that have adequate sensitivity and specificity to distinguish those who are likely to develop AD from those memory-impaired individuals who will not. The pathological hallmarks of AD are the deposition of senile plaques (SPs) and neurofibrillary tangles (NFTs) (Vickers et al., 2000). SPs and NFTs are mainly composed of β-amyloid (Aβ) protein and hyperphosphorylated tau protein, respectively. Aβ is a 4 kDa 39–43 amino acid metalloprotein product derived from the proteolytic cleavage of the amyloid precursor protein (APP) by β- and γ-secretases. The abnormal accumulation of SPs has been implicated as a central event in the etiology and the pathogenesis of AD and precedes the cognitive deterioration observed in AD (Okamura et al., 2008). Tau proteins accumulate in the neuronal cytoplasm and form NFTs with age. The initial lesions leading to NFTs occur in the transentorhinal cortex, followed by involvement of the entorhinal cortex and hippocampus, progressing to the neocortex. In vivo detection of SPs and NFTs in the brain enables the detection of AD patients in the pre-symptomatic stage. Noninvasive measurement of the amount of Aβ and tau deposits in the living brain is desirable for preventive interventions and assessment of therapeutic effects.

The density of SPs in brain tissue can be measured by molecular imaging techniques using positron emission tomography (PET) and a specific radiotracer. As Aβ deposits in the AD brain generally include the β-sheet fibrillar structure, many β-sheet binding agents have been developed as Aβ binding radiotracers for PET imaging. Currently, the most successful amyloid-binding agent is N-methyl-[$^{11}$C]2-(4'-methylaminophenyl)-6-hydroxybenzothiazol (PIB), which has been shown to possess a high affinity for Aβ fibrils. PIB-PET studies in human subjects have shown a robust difference between the retention pattern in AD patients and healthy controls, with AD cases showing significantly higher retention of PIB in the neocortical areas of the brain affected by Aβ deposition (Klunk et al., 2004). PIB retention in the neocortical areas is correlated with the Aβ plaque load (Ikonomovic et al., 2008). Benzoxazole derivatives are also promising alternatives for amyloid-imaging probes (Okamura et al., 2004; Furumoto et al., 2007). A PET study using $^{11}$C-labeled 2-(2-[2-dimethylaminothiazol-5-yl]ethenyl)-6-(2-[fluoro]ethoxy) benzoxazole (BF-227) demonstrated retention of this tracer in the cerebral cortices of AD patients but not in those of normal subjects. AD patients were clearly distinguishable from normal individuals using neocortical uptake of [$^{11}$C]BF-227 (Kudo et al., 2007). Neocortical retention of BF-227 was observed in the subjects with mild cognitive impairment (MCI). BF-227 PET showed higher specificity and sensitivity than FDG-PET and

voxel-based morphometric analysis of MRI for differentiating between AD patients and normal controls, and between MCI converters and non-converters (Waragai et al., 2009; Furukawa et al., 2010). A voxel-by-voxel analysis demonstrated a higher retention of [$^{11}$C]BF-227, mainly in the posterior association cortex of AD patients and MCI converters. This distribution pattern corresponds well with the distribution of neuritic plaque deposits in postmortem AD brains. These findings suggest that [$^{11}$C]BF-227 is a promising PET probe for in vivo detection of dense amyloid deposits in AD patients.

AD and many other neurodegenerative disorders, including frontotemporal dementia (FTD), progressive supranuclear palsy, corticobasal degeneration, Parkinson's disease (PD), dementia with Lewy bodies (DLB), multiple system atrophy, and prion disease, belong to the family of protein misfolding diseases characterized by protein self-aggregation and deposition (Table 1). The tissue deposits observed in the brain in these diseases usually contain an enriched β-sheet structure, suggesting a potential target for non-invasive imaging using β-sheet binding agents. Thus, molecular PET imaging has the potential to be extended to this wide spectrum of protein misfolding diseases (Okamura et al., 2005; Okamura et al., 2009). The purpose of this study was to evaluate the clinical utility of [$^{11}$C]BF-227 PET for the noninvasive detection of misfolded proteins in the brain.

## EXPERIMENT

### Subjects

[$^{11}$C]BF-227 PET study was performed in 12 elderly normal controls, 14 patients with Alzheimer's disease (AD) and 12 subjects with mild cognitive impairment (MCI). The [$^{11}$C]BF-227 PET study was additionally performed in patients with frontotemporal dementia (FTD), dementia with Lewy bodies (DLB), multiple system atrophy (MSA), sporadic *Creutzfeldt-Jakob disease* (sCJD) and *Gerstmann-Sträussler-Scheinker* disease (GSS). The MCI subjects were divided into two groups: MCI converters (n=6) and MCI non-converters (n=7). The MCI converters were defined as patients who eventually developed AD within a mean follow-up of 27.0±7.9 months (range 14–30 months). The MCI non-converters were defined as having a transient memory loss or remaining cognitively stable through at least a two-year follow-up (27.7±2.2 months; range 25–30 months).

*Table 1. Protein misfolding diseases and their fibrillar deposits*

| Protein | Fibrillar deposits | Diseases |
|---|---|---|
| Amyloid-β | Senile plaque<br>Cerebrovascular amyloid | Alzheimer's disease<br>Down syndrome<br>Cerebral amyloid angiopathy |
| Tau | Neurofibrillary tangle<br>Pick body<br>Tufted astrocytes<br>Astrocytic plaque | Alzheimer's disease<br>Frontotemporal lobar degeneration<br>Progressive supranuclear palsy<br>Corticobasal degeneration |
| α-synuclein | Lewy body<br>Glial cytoplasmic Inclusions | Parkinson's disease<br>Dementia with Lewy bodies<br>Multiple system atrophy |
| Prion | Prion plaque | Creutzfeldt-Jakob disease<br>Gerstmann-Sträussler-Scheinker disease |

## Method

[$^{11}$C]BF-227 was synthesized from its precursor by N-methylation in dimethyl sulfoxide using [$^{11}$C]methyl triflate, as previously described (Kudo et al., 2007). The [$^{11}$C]BF-227 PET study was performed using a SET-2400W PET scanner (Shimadzu, Kyoto, Japan). After intravenous injection of 211–366 MBq [$^{11}$C]BF-227, dynamic PET images were obtained for 60 min (23 sequential scans; 5 scans × 30 s, 5 scans × 60 s, 5 scans × 150 s, and 8 scans × 300 s) with closed eyes. The standardized uptake value (SUV) was calculated by normalizing tissue concentrations by injected dose and body weight. Regions of interest (ROIs) were placed on co-registered axial MR images. The ROI information was then copied onto the PET images, and regional SUV values were sampled. The ratio of regional SUV to cerebellar SUV (SUVR) between 40 and 60 min post administration was calculated as an index of [$^{11}$C]BF-227 retention. For the analysis of prion disease data, we calculated regional to pons SUV ratio (SUVRp). For the analysis of MSA patient data, the distribution volume of [$^{11}$C]BF-227 was calculated by Logan's graphical analysis using arterial blood sample data. The protocol of this study was approved by the Committee on Clinical Investigation at Tohoku University School of Medicine and by the Advisory Committee on Radioactive Substances at Tohoku University. Written informed consent was obtained from all patients and control subjects after a complete description of the study. The clinical study was performed in accordance with the Declaration of Helsinki.

## RESULTS

A PET study using [$^{11}$C]BF-227 demonstrated the retention of this tracer in the cerebral cortices of AD patients and MCI converters to AD but not in normal subjects or MCI non-converters (Figure 1). The average neocortical SUVR in BF-227 PET was significantly higher in the AD patients and MCI converters than in the normal subjects and MCI non-converters (Figure 2). We further examined BF-227 PET scans in patients with FTD, PD and DLB. Although imaging in FTD and PD patients showed normal distribution of BF-227 in the brain, DLB patients had moderate neocortical retention of BF-227 (Figure 1). Intriguingly, imaging from MSA patients showed BF-227 retention in the putamen, cerebral cortex and subcortical white matter. Microscopic examination indicates that BF-227 selectively binds to intracellular α-synuclein deposits, called glial cytoplasmic inclusions (GCIs), in MSA brain sections (Figure 3). Finally, significantly higher retention of BF-227 was detected in the cerebellum of GSS patients compared with that of normal controls and AD patients (Figure 4). In contrast, sCJD patients showed no obvious BF-227 retention in the cerebellum. Selective binding of BF-227 to prion protein plaques was confirmed using brain samples from autopsy-confirmed GSS cases (Figure 4).

## DISCUSSION

Our study demonstrated that [$^{11}$C]BF-227 PET is useful for the in vivo detection of Aβ and prion protein plaques in the human brain. BF-227 PET achieved high diagnostic accuracy in discriminating between MCI converters and non-converters. This result strongly suggests that [$^{11}$C]BF-227 PET would be useful to predict conversion from MCI to AD. Regarding the binding of PET imaging agents to prion proteins, a previous PET study demonstrated a moderate level of FDDNP retention and no remarkable PIB retention in the brain of familial CJD patients (Boxer et al., 2007). Another PET study also demonstrated that PIB was not specifically retained in two sCJD patients (Villemagne et al., 2009). In comparison with these previous studies, BF-227 successfully

*Figure 1. [$^{11}$C]BF-227 PET images in an elderly normal control, a patient with Alzheimer's disease (AD), a MCI non-converter, a MCI converter, a patient with frontotemporal dementia (FTD) and a patient with dementia with Lewy bodies (DLB).*

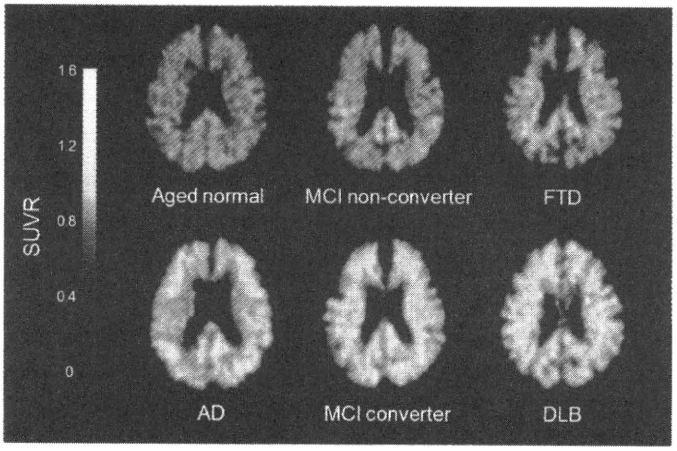


*Figure 2. Average neocortical SUVR values in elderly normal controls (AN), MCI non-converters (MCI-NC), MCI converters (MCI-C), and patients with Alzheimer's disease (AD). *$p<0.05$, ANOVA followed by a Bonferroni multiple comparisons test.*

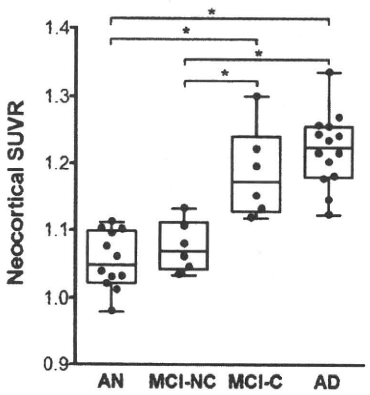


visualized prion protein plaques in the brains of GSS patients. Histopathological studies indicate a higher density of prion protein plaques in GSS patients than in familial CJD patients (Okamura et al., 2010). Therefore, the differences between our findings and those of previous studies would mainly depend upon the amount of prion protein fibrils in the brain. The difference might also be attributable to higher binding affinity of BF-227 to prion protein plaques compared to the other PET probes. Further analysis is necessary to compare the variable binding affinity of different PET probes for prion protein fibrils.

PET and microscopic studies also demonstrated that BF-227 has a potential ability to bind to and detect α-synuclein protein deposits in the brain. Previous PIB-PET studies have shown neocortical tracer accumulation in the brains of DLB patients. However, an in vitro binding study indicated that PIB failed to stain Lewy bodies in DLB brain sections. Considering the smaller size and lower density of Lewy bodies within the brains of DLB subjects relative to amyloid plaques, the contribution of Lewy bodies to the PET signals would be negligible. A recent study demonstrated that [$^{18}$F]BF-227 binds α-synuclein fibrils (Kd = 9.63 nM) with high affinity (Fodero-Tavoletti et al., 2009). Moreover, BF-227 labeled Lewy bodies and GCIs in fluorescence and immunohistochemical analyses of human brain sections, suggesting that BF-227 has higher binding affinity to α-synuclein deposits than PIB. Elevated BF-227 uptake was

*Figure 3. (A): [$^{11}$C]BF-227 PET images in a normal control subject (Control) and a patient with multiple system atrophy (MSA). (B and C): Microscopic images of BF-227 staining (B) and α-synuclein immunostaining (C) of the cerebellar white matter of a MSA case. Bar = 100 μm.*

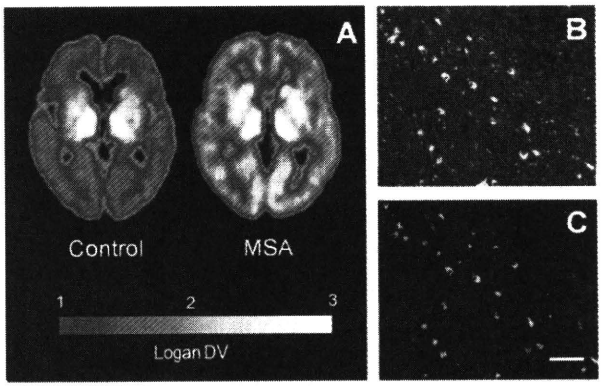


*Figure 4. (A): The regional to pons SUV ratio (SUVRp) values in the cerebella of 10 normal controls, 17 patients with Alzheimer's disease (AD), 2 patients with sporadic Creutzfeldt-Jakob disease (sCJD), and 3 patients with Gerstmann-Sträussler-Scheinker disease (GSS). (B and C): Microscopic images of BF-227 staining (B) and PrP immunostaining (C) of the cerebellar cortex of a GSS case. Bar = 25 μm.*

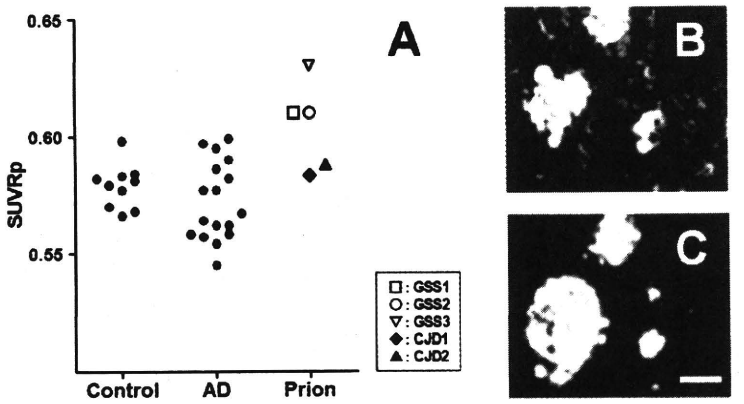


observed in the brains of MSA patients, which contain more α-synuclein deposits than those of DLB patients (Kikuchi et al., 2010). Further clinical studies of patients with α-synucleinopathy will clarify the potential of BF-227 for noninvasive detection of α-synuclein deposits in the human brain. From these findings, we conclude that BF-227 PET provides a potential method to facilitate both early diagnosis and noninvasive monitoring of protein misfolding diseases.

## ACKNOWLEDGMENT

Part of this study was supported by the Health and Labor Sciences Research Grants for Translational Research from the Ministry of Health and the

Grant-in-Aid for Scientific Research on Priority Areas, Integrative Brain Research, from the Ministry of Education, Culture, Sports, Science, and Technology of Japan (20019006). We appreciate the technical assistance of Dr. R. Iwata, Dr. S. Watanuki, M. Miyake and Dr. Y. Ishikawa in the clinical PET studies, and Dr. K. Sugi and Dr. S. He in the imaging analysis. We also thank Dr. M. Higuchi for supporting the staining of human brain sections.

## REFERENCES

Boxer, A. L., Rabinovici, G. D., Kepe, V., Goldman, J., Furst, A. J., & Huang, S. C. (2007). Amyloid imaging in distinguishing atypical prion disease from Alzheimer disease. *Neurology, 69*, 283–290. doi:10.1212/01.wnl.0000265815.38958.b6

Fodero-Tavoletti, M. T., Mulligan, R. S., Okamura, N., Furumoto, S., Rowe, C. C., & Kudo, Y. (2009). In vitro characterisation of BF227 binding to alpha-synuclein/Lewy bodies. *European Journal of Pharmacology, 617*, 54–58. doi:10.1016/j.ejphar.2009.06.042

Furukawa K., Okamura, N., Tashiro, M., Waragai, M., Furumoto, S., Iwata, R., ... Arai, H. (2010). Amyloid PET in mild cognitive impairment and Alzheimer's disease with BF-227: Comparison to FDG-PET. *Journal of Neurology*.

Furumoto, S., Okamura, N., Iwata, R., Yanai, K., Arai, H., & Kudo, Y. (2007). Recent advances in the development of amyloid imaging agents. *Current Topics in Medicinal Chemistry, 7*, 1773–1789. doi:10.2174/156802607782507402

Ikonomovic, M. D., Klunk, W. E., Abrahamson, E. E., Mathis, C. A., Price, J. C., & Tsopelas, N. D. (2008). Post-mortem correlates of in vivo PIB-PET amyloid imaging in a typical case of Alzheimer's disease. *Brain, 131*, 1630–1645. doi:10.1093/brain/awn016

Kikuchi, A., Takeda, A., Okamura, N., Tashiro, M., Hasegawa, T., Furumoto, S., ... Itoyama, Y. (2010). In vivo visualization of α-synuclein deposition by [$^{11}$C]-BF-227 PET in multiple system atrophy. *Brain*.

Klunk, W. E., Engler, H., Nordberg, A., Wang, Y., Blomqvist, G., & Holt, D. P. (2004). Imaging brain amyloid in Alzheimer's disease with Pittsburgh Compound-B. *Annals of Neurology, 55*, 306–319. doi:10.1002/ana.20009

Kudo, Y., Okamura, N., Furumoto, S., Tashiro, M., Furukawa, K., & Maruyama, M. (2007). 2-(2-[2-Dimethylaminothiazol-5-yl]ethenyl)-6-(2-[fluoro]ethoxy)benzoxazole: A novel PET agent for in vivo detection of dense amyloid plaques in Alzheimer's disease patients. *Journal of Nuclear Medicine, 48*, 553–561. doi:10.2967/jnumed.106.037556

Okamura, N., Fodero-Tavoletti, M. T., Kudo, Y., Rowe, C. C., Furumoto, S., & Arai, H. (2009). Advances in molecular imaging for the diagnosis of dementia. *Expert Opinion on Medical Diagnostics, 3*, 705–716. doi:10.1517/17530050903133790

Okamura, N., Furumoto, S., Arai, H., Iwata, R., Yanai, K., & Kudo, Y. (2008). Imaging amyloid pathology in the living brain. *Current Medical Imaging Reviews, 4*, 56–62. doi:10.2174/157340508783502840

Okamura, N., Shiga, Y., Furumoto, S., Tashiro, M., Tsuboi, Y., Furukawa, K., ... Doh-Ura, K. (2010). In vivo detection of prion amyloid plaques using [$^{11}$C]BF-227 PET. *European Journal of Nuclear Medicine and Molecular Imaging*.

Okamura, N., Suemoto, T., Furumoto, S., Suzuki, M., Shimadzu, H., & Akatsu, H. (2005). Quinoline and benzimidazole derivatives: Candidate probes for in vivo imaging of tau pathology in Alzheimer's disease. *The Journal of Neuroscience, 25*, 10857–10862. doi:10.1523/JNEUROSCI.1738-05.2005

Okamura, N., Suemoto, T., Shimadzu, H., Suzuki, M., Shiomitsu, T., & Akatsu, H. (2004). Styrylbenzoxazole derivatives for in vivo imaging of amyloid plaques in the brain. *The Journal of Neuroscience, 24*, 2535–2541. doi:10.1523/JNEUROSCI.4456-03.2004

Vickers, J. C., Dickson, T. C., Adlard, P. A., Saunders, H. L., King, C. E., & McCormack, G. (2000). The cause of neuronal degeneration in Alzheimer's disease. *Progress in Neurobiology, 60*, 139–165. doi:10.1016/S0301-0082(99)00023-4

Villemagne, V. L., McLean, C. A., Reardon, K., Boyd, A., Lewis, V., & Klug, G. (2009). $^{11}$C-PiB PET studies in typical sporadic Creutzfeldt-Jakob disease. *Journal of Neurology, Neurosurgery, and Psychiatry, 80*, 998–1001. doi:10.1136/jnnp.2008.171496

Waragai, M., Okamura, N., Furukawa, K., Tashiro, M., Furumoto, S., & Funaki, Y. (2009). Comparison study of amyloid PET and voxel-based morphometry analysis in mild cognitive impairment and Alzheimer's disease. *Journal of the Neurological Sciences, 285*, 100–108. doi:10.1016/j.jns.2009.06.005

## KEY TERMS AND DEFINITIONS

**Alzheimer's Disease:** The most common form of dementia.

**Mild Cognitive Impairment (MCI):** A diagnosis given to individuals who have cognitive impairments beyond that expected for their age and education but that do not interfere significantly with their daily activities.

**Neurofibrillary Tangles:** Pathological protein aggregates found within neurons in cases of Alzheimer's disease.

**Positron Emission Tomography (PET):** A nuclear medicine imaging technique that produces a three-dimensional image or picture of functional processes in the body.

**Prion:** An infectious agent that is primarily composed of protein.

**Protein Misfolding Diseases:** Clinically and pathologically diverse disorders in which specific proteins accumulate in cells or tissues of the body.

**Senile Plaques:** Extracellular deposits of amyloid in the gray matter of the brain.

**Tau:** A neuronal microtubule-associated protein found predominantly on axons.

**α-Synuclein:** The primary structural component of Lewy body fibrils.

**β-Amyloid:** A 39-43 amino acid peptide that appears to be the main constituent of senile plaques in the brains of Alzheimer's disease patients.